Available online at www.sciencedirect.com
ScienceDirect
Nuclear Physics B Proceedings Supplement 00 (2012) 1–6
Nuclear Physics B Proceedings Supplement

Heavy Flavour Production and Spectroscopy at LHCb

Patrizia de Simone
on behalf of the LHCb Collaboration

Laboratori Nazionali di Frascati, I.N.F.N., Via E. Fermi 40, 00044 Frascati (Rome) Italy

Abstract

The LHCb experiment has accumulated over 1 fb $^{-1}$ of data in proton-proton collisions at 7 TeV. These data provide samples rich in heavy flavoured hadrons, enabling a wealth of measurements to be made as well as probes of QCD theory predictions. We present recent results in quarkonium and b and c hadron production, as well as studies of these states' properties such as masses and decay asymmetries.

Keywords: hadron-hadron collision, charmonium, bottomonium, open charm, particle production, heavy flavour physics, spectroscopy

1. Introduction

The LHCb detector [1] has been designed for precision studies of CP violation and rare decays of heavy flavours at the Large Hadron Collider (LHC), at CERN. As the $b\bar{b}$ pairs are predominantly produced at small angles at high energies, the LHCb detector is a single forward arm spectrometer with an unique pseudo-rapidity acceptance of $1.9 < \eta < 4.9$.

The LHCb physics results on production and spectroscopy of heavy hadrons are complementary to those of the general pourpose detectors, and are essential to obtain complete and valuable tests of perturbative and non-perturbative QCD models. The data sample available for these studies is large: during the year 2011 the LHCb experiment accumulated over 1 fb $^{-1}$ of data at $\sqrt{s} = 7$ TeV, and the measured values of the charm and beauty production cross sections in the LHCb acceptance are:
$\sigma(c\bar{c})$= 1742 ±267 μb [2],
$\sigma(b\bar{b})$= 75.3 ±5.4 ± 13. μb [3].

All the results presented in this report have an uncertainty on the integrated luminosity of about 3.5% [4].

Table 1: *Production rates of prompt and non-prompt quarkonia at $\sqrt{s}$ = 7 TeV.*

$\sigma_{prompt}(J/\psi) = 10.52 \pm 0.04 \pm 1.40^{+1.64}_{-2.20}\ \mu b$ [5]
$\sigma(J/\psi) = 1.14 \pm 0.01 \pm 0.16\ \mu b$
$\sigma_{prompt}(\psi(2S)) = 1.44 \pm 0.01 \pm 0.12^{+0.20}_{-0.40}\ \mu b$ [6]
$\sigma(\psi(2S)) = 0.25 \pm 0.01 \pm 0.02\ \mu b$
$\sigma_{prompt}(Y(1S)) = 2.29 \pm 0.01 \pm 0.10^{+0.19}_{-0.37}\ nb$ [7]
$\sigma_{prompt}(Y(2S)) = 0.562 \pm 0.007 \pm 0.023^{+0.048}_{-0.092}\ nb$
$\sigma_{prompt}(Y(3S)) = 0.283 \pm 0.005 \pm 0.012^{+0.025}_{-0.048}\ nb$

2. Quarkonia

2.1. Charmonia and Bottomonium production

The quarkonia states J/ψ, $\psi(2S)$ and $Y(nS)$ are selected trought the decay channel $\mu^+\mu^-$. In the case of the $\psi(2S)$, the decay channel $\psi(2S) \rightarrow J/\psi\pi^+\pi^-$ is added, despite a larger background and a lower reconstruction efficiency, it is used to cross-check and to average the $\mu^+\mu^-$ result.

We measure the production cross sections of prompt and non-prompt charmonia. J/ψ and $\psi(2S)$ from b-hadron decays can be distinguished from promptly produced charmonia exploiting their finite decay time. The differential cross sections have been measured as a function of the transverse momentum p_T and of the rapidity y of the selected quarkonia states. The table 1 shows the cross sections integrated over the acceptance regions in p_T <~ 16 GeV/c and $2 < y < 4.5$. The prompt cross sections are evaluated assuming zero polarization, and the third uncertainty gives the deviation from the central value when the quarkonia states are either fully transversely or fully longitudinally polarized in the helicity frame.

Prompt production studies carried out at the Tevatron collider in the early 1990s [8] made clear that the Non Relativistic QCD calculations, based on the Leading Order (LO) Colour Singlet (CS) model, failed to describe the absolute value and the transverse momentum dependence of the charmonium production cross-sections and polarization data. On the other hand, recent QCD computations yielded predictions in better agreement with the experimental data.

To allow a comparison with the theory, the promptly produced quarkonia should be separated from those cascading from higher mass states (feed-down). As an example, fig 1 shows the differential cross-section for promptly produced $\psi(2S)$ mesons, which have not appreciable feed-down contribution, along with a comparison with some recent theory predictions [9] [10] [11] [12] tuned to the LHCb acceptance. The Fig. 1 shows that the experimental data on $\psi(2S)$ differential production cross section are well described by the Next Leading Order (NLO) calculation including CS and Color Octet (CO) models, but also by Next to Next Leading Order (NNLO) calculation including only CS models. J/ψ and $\psi(2S)$ from b-hadron decays are well described by QCD prediction based on Fixed Order Next to Leading Log (FONLL) approximitaion.

Since the beginning of 2012 LHCb is collecting data at $\sqrt{s}$ = 8 TeV, and allows to perform again all these measurements at the higher energy.

2.2. Double charm production

Recently, studies of double charmonium and charmonium with associated open charm production have been proposed as probes of the quarkonium production mechanism [13]. In pp collisions, additional contributions, such as Double Parton Scattering (DPS) or the intrinsic charm content of the proton to the total cross section, are allowed, though these constributions may not be mutually exclusive.

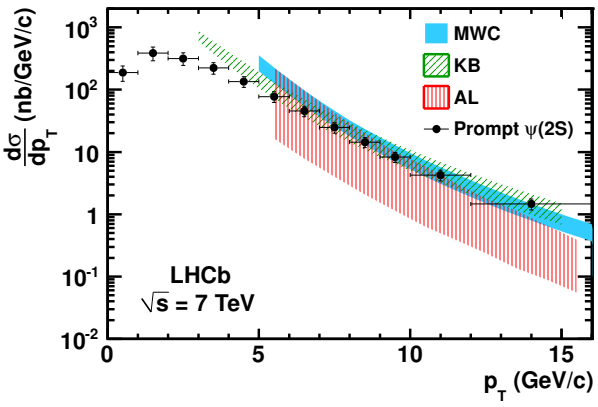

Figure 1: *Differential production cross-section vs. p_T for prompt $\psi(2S)$. The predictions of three nonrelativistic QCD models are also shown for comparison. MWC [9] and KB [10] are NLO calculations including CS and CO contributions. AL [11] [12] is a CS model including the dominant NNLO terms.*

The cross section for double J/ψ production, $\sigma_{J/\psi J/\psi}$, was measured in 2011 with an integrated luminosity of 38 pb^{-1} [15] by requiring two prompt $J/\psi \to \mu^+\mu^-$. The statistical significance of the double J/ψ signal is larger than 6σ. The analysis was performed in the acceptance region p_T <~ 10 GeV/c and $2 < y < 4.5$, and gave the result $\sigma_{J/\psi J/\psi} = 5.1 \pm 1.0 \pm 1.1$ nb. The result is consistent with LO calculations for the gluon fusion process, $gg \to J/\psi J/\psi$, in perturbative QCD, $\sigma^{gg}_{J/\psi J/\psi} = 4.1 \pm 1.2$ nb [16]. Moreover the LHCb result allows for a contribution from the DPS mechanism, $\sigma^{DPS}_{J/\psi J/\psi} = 2.\pm 1.$ nb [17], this could be better investigated with the full statistic collected at 7 TeV.

The production cross sections of J/ψ mesons associated with open charm and pairs of open cham hadrons have been oserved and studied with 355 pb $^{-1}$ [18]. Most of the channels are observed with a statistical significance larger than 5σ.
The measured cross sections are larger than the LO gluon fusion predictions [19] [20], while the DPS prediction [14] works nicely for the J/ψ open charm mode. These are the first observations of these kind of double charm events at hadron colliders.
New measurements and more channels ($J/\psi + \psi(2S)$, $J/\psi + Y(nS)$, $Y(nS) + Y(nS)$) will be explored with the full statistics at $\sqrt{s}$ = 7 TeV, and at $\sqrt{s}$ = 8 TeV.

2.3. Heavy Onia: $\sigma(\chi_{C1})/\sigma(\chi_{C2})$

The study of the production of P-wave charmonia χ_C is important since these resonances give substantial

feed-down contributions to the prompt J/ψ production through their radiative decay $\chi_C \to J\psi\gamma$, and can have significant impact on the measurement of the J/ψ polarization [1]. Furthermore the ratio $\sigma(\chi_{C1})/\sigma(\chi_{C2})$ is interesting because it is sensitive to the CS and CO production mechanisms. Prompt χ_C have been reconstructed through the decay chain $\chi_C \to J/\psi\gamma$, and $J/\psi \to \mu^+\mu^-$ in the acceptance region $2 < p_T(J/\psi) < 16$ GeV/c and $2 < y(J/\psi) < 4.5$ using 36 pb $^{-1}$ of data [21]. The yields of the three onia states [2] is obtained with an unbinned maximum likelihood fit to the mass difference distribution between the combination $\mu^+\mu^-\gamma$ and $\mu^+\mu^-$. Fig. 2 shows the ratio $\sigma(\chi_{C1})/\sigma(\chi_{C2})$ as a function of $p_T(J/\psi)$. The left hatched band shows the result of

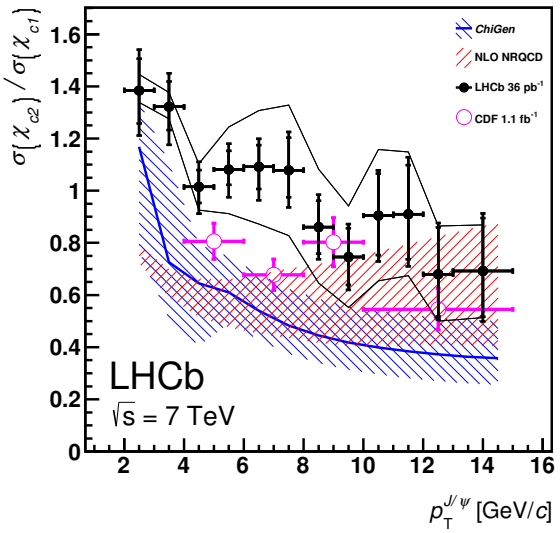

Figure 2: Ratio $\sigma(\chi_{C1})/\sigma(\chi_{C2})$ as a function of $p_T(J/\psi)$. The LHCb results, assuming the production of unpolarised χ_C mesons, are shown with solid black circles. The lines surrounding the data points show the maximum effect of the unknown χ_C polarisations on the result. The CDF data points, at $\sqrt{s}$=1.96 TeV, are shown with open circles [22]. The two hatched bands correspond to the ChiGen Monte Carlo generator prediction [23] and NLO NRQCD [24].

the NLO NRQCD [24] calculations in reasonable agreement with the data for $p_T(J/\psi) > 8$ GeV/c, whilst there is a discrepancy at low $p_T(J/\psi)$. Although the *ChiGen* generator [23] describes the shape reasonably well, the data lie consistently above the theory prediction. This could be explained by important higher order perturbative corrections and/or sizeable colour octet terms not included in the calculation.

[1] The quarkonia polarization measurements are ongoing analysis at LHCb.

[2] Since the BR($\chi_C 0 \to J/\psi\gamma$) is $\simeq$ 30 times smaller than those of χ_{C1} and χ_{C2}, the yield of χ_{C0} is not significant.

3. c hadrons

3.1. $D_s^+ - D_s^+$ production asymmetry

The production asymmetry between positive and negative D_s, together with the charge asymmetry in detection efficiency, is an important piece of information to measure CP asymmetries at LHCb. LHCb measured the $D_s^\pm$ prompt production cross section asymmetry, $A_p = \frac{\sigma(D_s^+)-\sigma(D_s^-)}{\sigma(D_s^+)+\sigma(D_s^-)}$, selecting the decays $D_s^\pm \to \phi(K^+K^-)\pi^\pm$ in a data sample of 1 fb $^{-1}$ [25]. Since $D_s^\pm \to \phi(K^+K^-)\pi^\pm$ is a Cabibbo favoured decay, no significant CP asymmetry is expected. Assuming it to be vanishing, A_p is determined after correcting for the relative D_s^+ and D_s^- detection efficiencies. In addition, since the final states are symmetric in kaon production, this requires only knowledge of the relative π^+ and π^- detection efficiencies, $\epsilon(\pi^+)/\epsilon(\pi^-)$.

In order to measure $\epsilon(\pi^+)/\epsilon(\pi^-)$, we use the decay sequence $D^{*+} \to \pi^+ D^0$, $D^0 \to K^-\pi^+\pi^-\pi^+$, and its charge-conjugate decay. Assuming that the D^* comes from the primary vertex (PV) there are sufficient kinematic constraints to reconstruct the decay even if one π from D^0 is omitted. We call these *partially* reconstructed decays. We can also *fully* reconstruct these decays. The ratio of *fully* to *partially* reconstructed decays provides a measurement of $\epsilon(\pi^+)/\epsilon(\pi^-)$ directly from the data sample. We examine D^{*+} and D^{*-} candidate decays separately, and also magnet up data separately from magnet down data, to test for possible left-right asymmetries of the detector.

All three candidate tracks ($K^+K^-\pi^\pm$) from the $D_s^\pm$ must form a common vertex that is detached from the primary one. Then the reconstructed momentum of the $D_s^\pm$ must point to the PV, to reduce to few percent the contamination from D produced in b hadron decays. A binned maximum likelihood fit gives the $D_s^\pm$ yields. The production asymmetry measured in the acceptance region $p_T > 2$ GeV/c and $2 < y < 4.5$ is consistent with the theory predictions [26] [27]:
$A_p = (-0.33 \pm 0.22 \pm 0.10)\%$.

4. b hadrons

4.1. $B^\pm$ production

The study of the $b\bar{b}$ production cross section is a powerful test of perturbative quantum chromodynamics (pQCD) calculations. These are available at NLO

[28] and with the FONLL [29] [30] approximations. In the NLO and FONLL calculations, the theoretical predictions have large uncertainties arising from the choice of the renormalisation and factorisation scales and the b-quark mass [31].

Accurate measurements provide tests of the validity of the different production models. LHCb performed the first measurement of $B^{\pm}$ production cross section in the forward region at protons collider, using 35 pb^{-1} [32]. The $B^{\pm}$ mesons are reconstructed exclusively selecting the $B^{\pm} \to J/\psi(\mu^+\mu^-)K^{\pm}$ decays. The integrated cross section in the acceptance region $2 < y < 4.5$ and $p_T < 40$ GeV/c, is:
$\sigma(pp \to B^{\pm}X) = 41.1 \pm 1.5 \pm 3.1\mu$ b.

We plan to update this measurement with the full data sample collected at $\sqrt{s} = 7$ TeV, and to measure the production cross sections of the neutral mesons, B_d and B_s.

4.2. First observation of $B_c^+ \to J/\psi\pi^+\pi^-\pi^+$

Studies of the properties of the B_c meson are important, since it is the only meson consisting of two different heavy quarks. It is also the only meson in which decays of both constituents compete with each other. LHCb observed the decay $B_c^+ \to J/\psi\pi^+\pi^-\pi^+$ using a data sample corresponding to an integrated luminosity of 0.8 fb $^{-1}$ [33]. The branching fraction for this decay is expected to be 1.5 - 2.3 times higher than the BR($B_c^+ \to J/\psi\pi^+$) [34] [35]. However, the larger number of pions in the final state results in a smaller total detection efficiency due to the limited detector acceptance. We measure the branching ratio of the decay $B_c^+ \to J/\psi\pi^+\pi^-\pi^+$ relatively to BR($B_c^+ \to J/\psi\pi^+$) :

$$\frac{BR(B_c^+ \to J/\psi\pi^+\pi^-\pi^+)}{BR(B_c^+ \to J/\psi\pi^+)} = 2.41 \pm 0.30 \pm 0.33$$

This result is in agreement with the theoretical predictions. The main contribution to the systematic error, $\simeq 9\%$, is due to the assumptions on the decay structure assumed in the simulation.

4.3. Orbitally excited B^{**} mesons

The properties of the excited B mesons containing a light quark are predicted by Heavy Quark Effective Theory (HQET) in the limit of infinite b-quark mass [36] [37]. Under the heavy quark approximation the B mesons are characterized by three quantum numbers: the orbital angular momentum L, the angular momentum of the light quark $j_q = |L \pm 1/2|$, and the total angular momentum $J = |j_q \pm 1/2|$. For L = 1 there are four different possible $(J; j_q)$ combinations, all parity-even. These are known as the orbitally excited states or B^{**} states. Among these states we have the $B_1(5721)^0$ and $B_2^*(5747)^0$, observed in $B^{*+}\pi$ and $B^+\pi$ decays [38]. With an integrated luminosity of 336.5 pb $^{-1}$, we reconstruct these decay modes, but also the $B^0\pi^+$ and $B^{*0}\pi^+$ modes, where we must observe the isospin partners of the mentioned states [39].

The soft γs from the B^{*0} decay are not reconstructed, therefore objects decaying to both $B^{*0}\pi^+$ and $B^0\pi^+$ are expected to show two peaks in the $B^0\pi^+$ invariant mass distribution. The B mesons are reconstructed in the $J/\psi(\mu^+\mu^-)K^*(892)^0(K^+\pi^-)$, $D^-\pi^+$, $D^-(K^+\pi^-\pi^-)\pi^+\pi^+\pi^-$. For convenience, we study the invariant mass relative to the threshold, which has the form $Q(B^0\pi^+) = M(B^0\pi^+) - M(B^0) - M(\pi^+)$, where $M(B^0)$ and $M(\pi^+)$ are the masses quoted by [40].

The signal resonances in the Q-distribution are modeled using relativistic Breit-Wigner lineshapes. The detector resolution is about 3 MeV/c^2 and can be safely neglected. The fit results are shown in Fig. 3. This

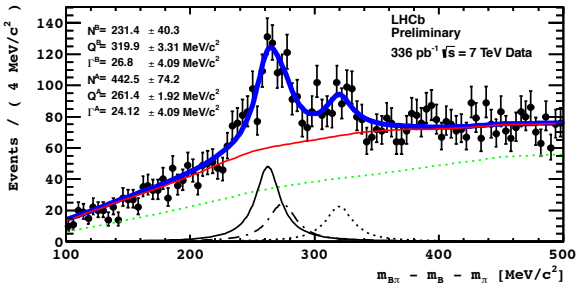

Figure 3: $Q(B^0\pi^+)$ distribution. LHCb data (points) and the total fit are superimposed. The components of the PDF are, combinatorial background and associated production, combinatorial background, $B_1^+ \to B^{*0}\pi^+$ (solid line), $B^{*+} \to B^{*0}\pi^+$ (dot-dashed line), and $B^{*+} \to B^0\pi^+$ (dotted line).

is the first observation of the decays $B_1^+ \to B^{*0}\pi^+$ and $B^{*+} \to B^0\pi^+$ with a significance of respectively 9.9 σ and 4.0 σ. The mass values are
$M(B_1^+) = (5726.3 \pm 1.9 \pm 3.0 \pm 0.5)$ MeV/c^2
$M(B^{*+}) = (5739.0 \pm 3.3 \pm 1.6 \pm 0.3)$ MeV/c^2, where the third error is due to the uncertainty on the B^0 mass. These masses are compatible with the masses of the corresponding isospin partners B^0 and B^{*0}.

4.4. First observation of excited b baryons

The quark model predicts the existence of two orbitally excited states Λ_b^{*0} with quantum numbers $J^P = 1/2^-, 3/2^-$, that are expected to decay to $\Lambda_b^0\pi^+\pi^-$ or to

$\Lambda_b^0\gamma$ depending on the mass of the excited states. The properties of the Λ_b^{*0} are described by several models [41] that predict mass values between the $\Lambda_b^0\pi^+\pi^-$ and the $\Sigma_b\pi$ thresholds.

We search for the excited Λ_b^{*0} baryons starting from the recontruction of Λ_b^0 baryons through the decay chain $\Lambda_b^0 \to \Lambda_c^+\pi^-$ and $\Lambda_c^+ \to pK^-\pi^+$. The selected sample from 1 fb^{-1} is large (70540±330) and clean (S/B $\simeq$ 11), and the background composition is well understood [42]. Combining the Λ_b^0 baryons with two oppositely charged pions coming from the same vertex, we reconstruct the total invariant mass to look for the existence of the predicted Λ_b^{*0} baryons [43]. The background model is extracted from the study of wrong-sign $\Lambda_b^0\pi^+\pi^+$ combinations. Figure 4 shows two narrow peaks slight above the $\Lambda_b^0\pi^+\pi^-$ threshold. The two new

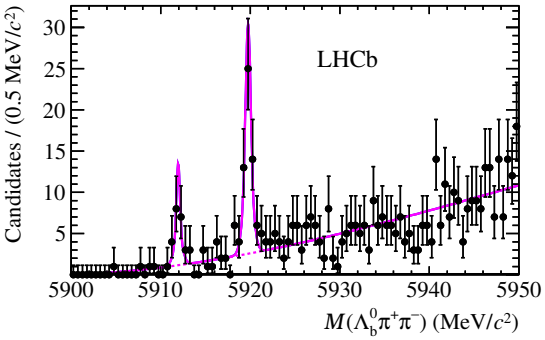

Figure 4: Invariant mass spectrum of $\Lambda_b^0\pi^+\pi^-$ combinations. The points with error bars are the data, the solid line is the fit result, the dashed line is the background contribution.

states are interpreted as the $1/2^-$ and $3/2^-$ orbital excitations of the ground state Λ_b^0, and were found to have masses of

$M(\Lambda_b^{*0}(1/2^-)) = 5911.95 \pm 0.12 \pm 0.03 \pm 0.66$ MeV/c^2,
$M(\Lambda_b^{*0}(3/2^-)) = 5919.76 \pm 0.07 \pm 0.02 \pm 0.66$ MeV/c^2,

the third error is due to the uncertainty on the Λ_b^0 mass. Because of the good mass resolution, order of 0.2 Mev/c^2, we were able to set upper limits on the natural widths $\Gamma(\Lambda_b^{*0}(1/2^-)) < 0.82$ MeV and $\Gamma(\Lambda_b^{*0}(3/2^-)) < 0.71$ MeV.

4.5. *b baryon decays to $D^0p\pi^-$ and D^0pK^-*

With a data sample of 330 fb $^{-1}$ we have reconstructed the $D^0p\pi$ and D^0pK invariant mass spectra, with $D^0 \to K\pi^+$ [44]. The yield of the Cabibbo suppressed decay channel $\Lambda_b^0 \to D^0pK^-$ is expected to be rather low, therefore channels with higher yields are needed to control potential systematic effects. We use the kinematically similar Cabibbo-favoured $\Lambda_b^0 \to D^0p\pi^-$ decay as well as the well established channel $\Lambda_b^0 \to \Lambda_c^+\pi^-$. The strategy is to measure first the rate of final states into $D^0p\pi^-$ respect to those into $\Lambda_c^+\pi^-$, then we determine the ratio of branching ratios:

$$R_{D^0pK^-} = \frac{BR(\Lambda_b^0 \to D^0pK^-)}{BR(\Lambda_b^0 \to D^0p\pi^-)} = 0.112 \pm 0.019^{+0.0011}_{-0.0014}$$

This is the first observation of Cabibbo suppressed decay $\Lambda_b^0 \to D^0pK^-$, with a significance of 6.3 σ. In addition, the D^0pK^- spectrum (Fig. 5), gives the hint of the presence of the neutral beauty strange baryon Ξ_b^0 with a significance of 2.6 σ, including the systematic effects.

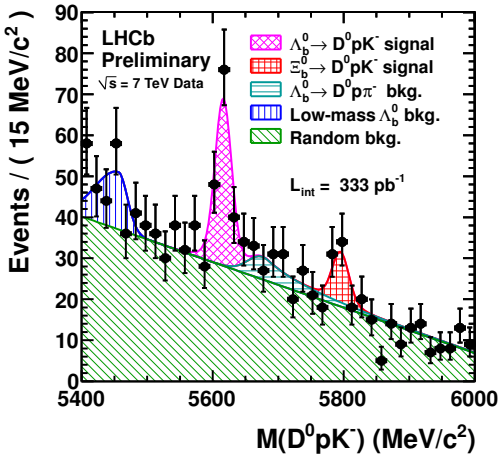

Figure 5: D^0pK^- invariant mass spectra and result of the corresponding fit. Points with error bars are the data, hatched areas are the different components in the fit model as detailed in the legend.

4.6. *Mass of the Ξ_b^- and Ω_b^- ground states*

With a data sampe of 620 pb $^{-1}$ we have measured the masses of the strange b-baryons Ω_b^- and Ξ_b^- [45], which are selected via the decay chains $J/\psi\Omega^-(\Lambda^0K^-)$ and $J/\psi\Xi^-(\Lambda^0\pi^-)$, respectively, with $J/\psi \to \mu^+\mu^-$ and $\Lambda^0 \to p\pi^-$. The mass measurement of the Ω_b^- is of particular interest, since the values reported for this state by the CDF and D0 collaborations are inconsistent at the 6 σ level [46]. Both decays share a similar topology and the presence of longlived particles and multiple vertices in the decay chain is exploited in the selection process. High background levels are observed near the interaction point, mainly from inclusive J/ψ production, thus we reconstruct only candidates with lifetime above 0.3 ps. The invariant mass distributions for the selected Ω_b^- and Ξ_b^- candidates are shown in Fig. 6. The mass

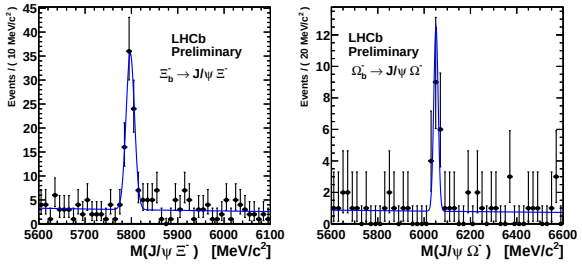

Figure 6: The invariant mass distributions for the selected Ξ_b^0 (left) and Ω_b^- (right) candidates. The fit projection is overlaid.

values are extracted performing an unbinned maximum likelihood fit. The results are
$M(\Xi_b^-) = 5796.5 \pm 1.2 \pm 1.2$ MeV/c^2,
$M(\Omega_b^-) = 6050.3 \pm 4.5 \pm 2.2$ MeV/c^2,
the systematic uncertainties are dominated by the momentum scale calibration. These results correspond to the best measurements of these masses to date. The measured Ω_b mass is compatible with the CDF measurement $M(\Omega_b^-) = 6054.4 \pm 6.9$ MeV/c^2.

5. Conclusion

In addition to the measurements reported here, there are other recent results from LHCb. Among these, we would like to mention the study of the heavy quarkonia states χ_b through the radiative decays $\chi_{bJ}(nP) \to Y(1S)\gamma$ [47] [48], the study of the exotic quarkonia states $X(3827)$ and $X(4140)$ [49] [50], and the spectroscopy studies of D_{sJ} [51].

LHCb has a world class heavy flavour production and spectroscopy program, and will continue to provide precise and competitive measurements.

References

[1] The LHCb Collaboration, JINST 3 (2008) S08005.
[2] The LHCb Collaboration, LHCb-CONF-2010-013.
[3] The LHCb Collaboration, Phys. Lett. B 694 (2010) 209-216.
[4] The LHCb Collaboration, R. Aaij, et al., J. Instrum. 7 (2012) P01010.
[5] The LHCb Collaboration, Eur. Phys. J. C 71 (2011) 1645.
[6] The LHCb Collaboration, Eur. Phys. J. C 72 (2012) 2100
[7] The LHCb Collaboration, Eur. Phys. J. C 72 (2012) 2025.
[8] CDF collaboration, Phys. Rev. Lett. 69 (1992) 3704.
[9] Y. Q. Ma, K. Wang and K. T. Chao, arXiv:hep-ph/1012.1030.
[10] B. Kniehl and M. Butensch on, Phys. Rev. Lett. 106 (2011) 022003, and private communication.
[11] P. Artoisenet et al., Phys. Rev. Lett. 101 (2008) 152001.
[12] J.P. Lansberg, Eur. Phys. J. C61 (2009) 693.
[13] S. J. Brodsky and J. P. Lansberg, Phys. Rev. D81 (2010) 051502, arXiv:hep-ph/0908.0754.
[14] The CDF collaboration, Phys. Rev. D56 (1997) 3811.
[15] The LHCb Collaboration, Phys. Lett. B707 (2011) 52.
[16] A. V. Berezhnoy, A. K. Likhoded, A. V. Luchinsky, and A. A. Novoselov, Phys. Rev. D84 (2011) 094023
[17] Novoselov,Tech. Rep. arXiv:1106.2184(2011).
[18] The LHCb Collaboration, JHEP 2012(06)(2012) 141.
[19] A. V. Berezhnoy, V.V. Kiselev, A. K. Likhoded, A.I. Onishchenko, Phys. Rev. D 57(1998) 4385.
[20] S. Baranov, Phys. Rev. D 73 (2006) 074021.
[21] The LHCb Collaboration, Phys. Lett. B 714 (2012) 215.
[22] The CDF collaboration, Phys. Rev. Lett. 98 (2007) 232001, [arXiv:hep-ex/0703028].
[23] L. A. Harland-Lang, and W. J. Stirling, http://projects.hepforge.org/superchic/chigen.html .
[24] Y.Q. Ma, K. Wang, K.T. Chao, Phys. Rev. D 83 (2011) 111503.
[25] The LHCb Collaboration, Phys. Lett. B 713 (2012) 186.
[26] M. Chaichain, and A. Fridman, Phys. Lett. B 298 (1993) 218.
[27] E. Norrbin, and T. Sjostrand, Eur. Phys. J. C 17 (2000) 137.
[28] P. Nason, S. Dawson and R.K. Ellis, Nucl. Phys. B 303 (1988) 607.
[29] M. Cacciari, M. Greco and P. Nason, JHEP 05 (1998) 007 [hep-ph/9803400]
[30] M. Cacciari, S. Frixione and P. Nason, JHEP 03 (2001) 006 [hep-ph/0102134].
[31] M. Cacciari, S. Frixione, M. Mangano, P. Nason and G. Ridolfi, JHEP 07 (2004) 033 [hep-ph/0312132].
[32] The LHCb Collaboration, JHEP 04 (2012) 093.
[33] The LHCb Collaboration, arXiv:1204.0079.
[34] A. Rakitin and S. Koshkarev, Phys. Rev. D81 (2010) 014005, arXiv:0911.3287.
[35] A. K. Likhoded and A. V. Luchinsky, Phys. Rev. D81 (2010) 014015, arXiv:0910.3089.
[36] S. Godfrey and N. Isgur, Phys. Rev. D32 (1985) 189. S. Godfrey and R. Kokoski, Phys. Rev. D43 (1991) 1679. N. Isgur and M.B. Wise, Phys. Rev. Lett. 66 (1991) 1130. M. Di Pierro and E. Eichten, Phys. Rev. D64 (2001) 114004.
[37] E. Eichten, C.T. Hill and C. Quigg, Phys. Rev. Lett. 71 (1993) 4116. A.F. Falk and T. Mehen, Phys. Rev. D53 (1996) 231.
[38] CDF Collaboration, Phys. Rev. Lett. 102 (2009) 102003. D0 Collaboration, Phys. Rev. Lett. 99 (2007) 172001.
[39] LHCb Collaboration, LHCB-CONF-2011-053.
[40] J. Beringer et al. (Particle Data Group), Phys. Rev. D86, 010001 (2012).
[41] S. Capstick and N. Isgur, Phys. Rev. D 34 (1986) 2809. Z. Aziza Baccouche, C. K. Chow, T. D. Cohen and B. A. Gelman, Nucl. Phys. A 696 (2001) 638. H. Garcilazo, J. Vijande and A. Valcarce, J. Phys. G G 34 (2007) 961. D. Ebert, R. N. Faustov and V. O. Galkin, Phys. Lett. B 659 (2008) 612. W. Roberts and M. Pervin, Int. J. Mod. Phys. A 23 (2008) 2817. M. Karliner, B. Keren -Zur, H. J. Lipkin and J. L. Rosner, Annals Phys. 324 (2009) 2. S. Narison and R. Albuquerque, Phys. Lett. B 694 (2010) 217. R. M. Albuquerque, S. Narison and M. Nielsen, Phys. Lett. B 684 (2010) 236.
[42] The LHCb Collaboration, LHCB-CONF-2011-036.
[43] The LHCb Collaboration, arXiv:1205.3452 [hep-ex].
[44] The LHCb Collaboration, LHCB-CONF-2011-036.
[45] The LHCb Collaboration, LHCB-CONF-2011-060.
[46] The D0 Collaboration, Phys. Rev. Lett. 101 (2008) 232002. The CDF Collaboration, Phys. Rev. D80 (2009) 072003.
[47] The LHCb Collaboration, LHCB-PAPER-2012-015.
[48] The LHCb Collaboration, LHCB-CONF-2012-020.
[49] The LHCb Collaboration, EPJC 72 (2012) 1972.
[50] The LHCb Collaboration, Phys. Rew. D 85 (2012) 091103.
[51] The LHCb Collaboration, LHCB-PAPER-2012-016. arXiv:1207.6016(2012).